SolarPACES 2023, 29th International Conference on Concentrating Solar Power, Thermal, and Chemical Energy Systems

Analysis and Simulation of CSP and Hybridized Systems

https://doi.org/10.52825/solarpaces.v2i.908

Published: 28 Aug. 2024

Dynamic Modeling of a Thermochemical System for Solar Fuel Production Based on an Open-Source Framework

Falko Schneider[1], Christian Schwager[1], Cristiano José Teixeira Boura[1], Nico Oellers[1], Alfonso Villegas[2], and Ulf Herrmann[1]

[1] Solar-Institute Jülich of FH Aachen University of Applied Sciences, Germany

[2] Synhelion SA, Lugano, Switzerland

Abstract. This paper describes the dynamic process model for a solar fuels synthesis plant currently being built in Germany. The open-source, equation-based modelling language Modelica is used as the foundation. In this plant, biogas and steam are reformed, producing synthesis gas and subsequently turned into synthetic crude oil. This work contains the necessary model setups for the thermal energy storage, solar-absorbing gas receiver and reforming reactor to consider the thermohydraulic, thermochemical and radiative interactions occurring in the process. The remaining infrastructure is modeled with the Modelica Standard Library. A way to fit these models with experimental data for validation is also outlined.

Keywords: Dynamic Simulation, Modelica, Solar Fuels, Thermochemical Equilibrium, Dry Reforming, Steam Reforming, Concentrated Solar Power (CSP), Solar-Absorbing Gas Receiver

1. Introduction

Concentrated solar power (CSP) applications, primarily providing heat for chemical applications instead of electrical power, are expanding fast. One of those applications is the production of solar fuels, where the solar heat is used to reform biogas and steam, producing synthesis gas (syngas) to subsequently create synthetic crude oil. The main goal is to provide a sustainable liquid fuel for industries that rely on its high energy density, e.g. the aviation industry. The construction of an industrial-scale pilot plant implementing that process has begun in Jülich (Germany) in 2023.

Controlling CSP power generation plants is challenging due to the volatile solar energy input. This challenge is even more significant for the application presented in this work because the reforming process and its chemical reactions are integrated into the system, and its efficiency and output composition must be controlled precisely. Dynamic simulations have proven advantageous for investigating CSP systems and developing optimized control strategies [1, 2]. This paper describes a dynamic process model based on an open-source framework, which applies this approach to the described thermochemical system.

2. Plant & Model Setup

Figure 1 shows the CSP cycle with a solar absorbing gas receiver (SAGR), a fan, a reformer and a thermal energy storage (TES) to enable sun-independent operation. Depending on the plant operating mode, the SAGR and/or TES superheat a steam flow as heat transfer fluid (HTF) from around 700 °C to 1200 °C, supplying necessary sensible and reaction heat to the reformer. On the chemical reaction side of the plant, steam and biogas are compressed, mixed and preheated on the reforming line and subsequently react to syngas inside the reformer using the heat supplied by the CSP cycle. The resulting product stream is cooled down via a heat recovery steam generator, which provides the reactant steam once the plant is in operation. After some treatment steps, synthetic crude oil is produced from the syngas using a Fischer-Tropsch process. This crude oil can be processed on-site or fed into the existing conventional refining industry for fossil fuels.

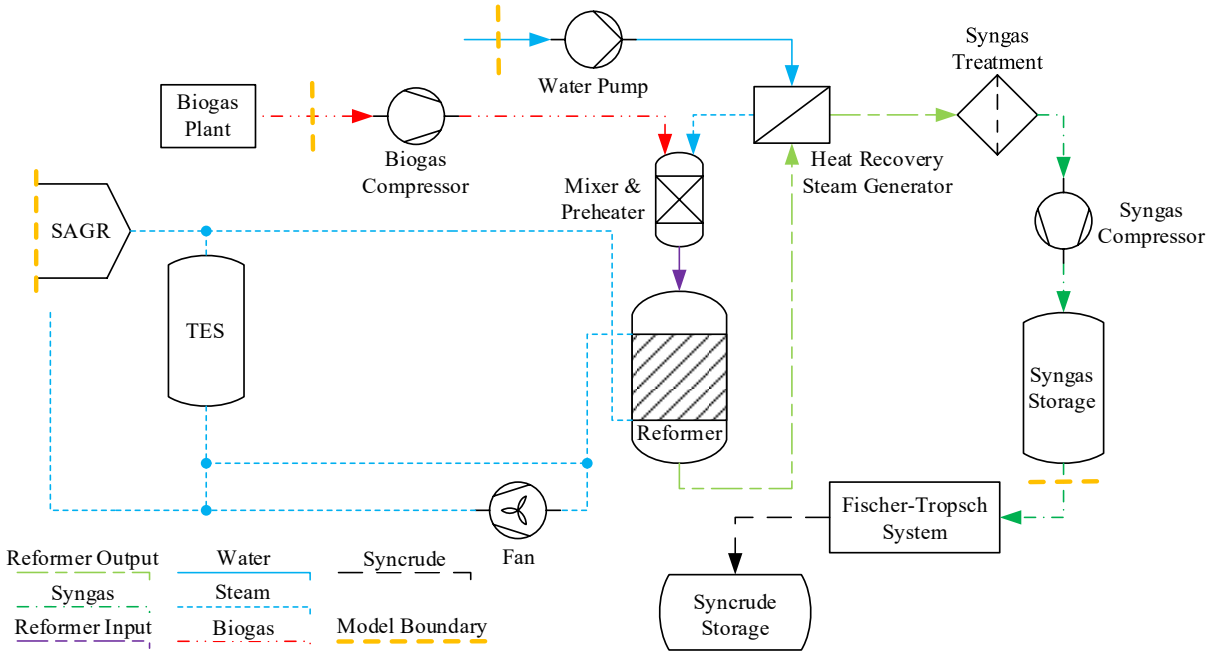

Figure 1. *Simplified model setup of the solar reforming process.*

The syngas storage is a buffer between the reforming line and the Fischer-Tropsch process. Thus, the Fischer-Tropsch process can be simulated independently using DWSIM, an open-source chemical process simulator, because the results do not affect the dynamic process model. Therefore, a feedback loop of the results is not necessary. The plant's infrastructure, i.e. valves, medium storages, pumps and piping, can be dynamically modeled with components from the Modelica Standard Library. They can be customized according to the specifications and operating characteristics of the components. All dynamic models can be built within an open-source environment like OpenModelica. However, the standard libraries lack the modeling basis for chemical reactions inside the reformer, mainly the steam reforming, dry reforming and reverse water gas shift reactions. Without this, the output temperature and composition of the reformer cannot be determined because the heat supplied by the CSP cycle provides not only the preheating of the educts but also the necessary reaction enthalpies. These calculation results are required downstream of the reformer, e.g. to calculate the heat recovery, which affects the reformer inlet conditions and, thereby, the heat sink in the CSP cycle. Each custom and standard library model contains ports so they can be interconnected to exchange information regarding the medium flows across their boundaries (cf. Figure 1), i.e. specific enthalpy, mass flow rate, pressure, medium model and composition.

2.1 Thermal Energy Storage Model

The TES used in the plant is a ceramic-based storage with solid bricks containing ducts for the HTF to flow through and exchange heat with the storage material. Because Modelica, by default, only enables differentiation with respect to time, the entire TES is spatially discretized into smaller cuboid cells. They are connected to create a TES model with a three-dimensional temperature profile. The degree of discretization, i.e. the resolution, is a trade-off between accuracy and computational effort. To model these volumes, the thermal conduction inside the material, the heat transfer between the HTF and the storage medium, the pressure drop in the HTF flow through the ducts and the resulting storage material temperature need to be determined for each one (cf. Figure 2).

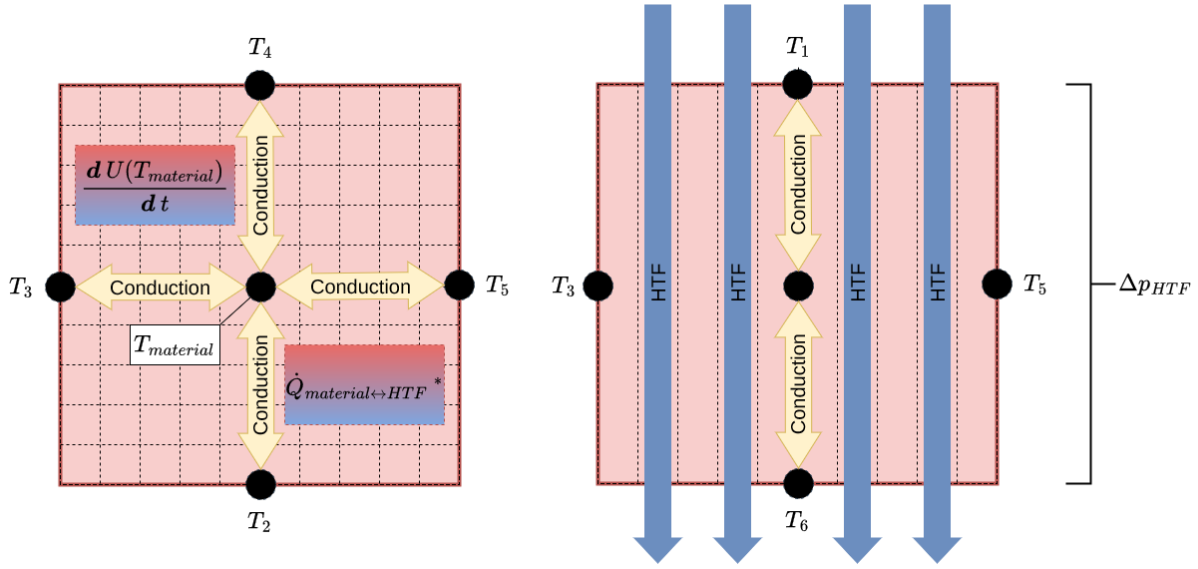

Figure 2. *Top-down (left) and lateral (right) conceptual diagram of a TES cell*

Each storage volume is modeled as a lumped thermal mass at the material temperature and is attributed to six boundary temperatures, which are coupled via the conduction inside each element (cf. Eq. 1). The heat losses to the environment are modeled via insulation elements, which are connected to the outer cells. The thermal conduction is calculated along the cuboid axes between each boundary surface and the center of the cell. Depending on the geometrical parameters of the ducts, the cross-sectional area of the heat-conducting material A_{cross} and the perpendicular length to the center L varies for each axis and boundary surface.

$$\dot{Q}_{conduction} = \sum_{i=1}^{6} \left((T_i - T_{material}) \cdot \frac{A_{cross,i} \cdot \lambda_{material}}{L_i} \right) \quad (1)$$

These ducts can have various geometries, but generally, the ratio of the duct width d_h and the wall thickness t_{wall} between two ducts is very high. This results in a high surface-to-volume ratio of the TES and thereby a higher heat transfer. Assuming a square duct and a square TES crosssection with a total number of ducts n_{ducts}, the heat-conducting area can then be simplified:

$$A_{cross,2} = A_{cross,3} = A_{cross,4} = A_{cross,5} = \sqrt{n_{ducts}} \cdot t_{wall} \cdot (L_1 + L_6) \quad (2)$$

The heat transfer between HTF and storage material is calculated for a single duct with a developed laminar flow via a Nusselt correlation [3] under the assumption of a constant heat transfer coefficient and wall temperature. The wall temperature is assumed to equal the material temperature since the material thickness between ducts is generally kept small to maximize the heat-exchanging surface to storage volume ratio. It is applied to the entire storage cell considering the heat transfer surface of each duct A_{duct}. The total surface depends

on the number of ducts in the cell n_{ducts}, i.e. the degree of discretization. Thus, the heat transfer couples the lumped thermal mass with the average HTF temperature. The HTF properties are calculated at the average HTF temperature T_{HTF} and pressure p_{HTF}.

$$\dot{Q}_{material \leftrightarrow HTF} = n_{ducts} \cdot A_{duct} \cdot \alpha \cdot \Delta T = n_{ducts} \cdot A_{duct} \cdot \frac{Nu \cdot \lambda_{HTF}}{d_h} \cdot (T_{material} - T_{HTF}) \quad (3)$$

An energy balance for the lumped mass with the mass $m_{material}$ and the heat capacity $c_{p,material}$ yields the time derivative of the storage material temperature $T_{material}$:

$$m_{material} \cdot c_{p,material} \cdot \frac{dT_{material}}{dt} = \dot{Q}_{material \leftrightarrow HTF} + \dot{Q}_{Conduction} \quad (4)$$

The pressure drop dp_{HTF} is calculated for the entire length of a single duct with the HTF mass flow rate $\dot{m}_{HTF}$ through the cell, dynamic viscosity η_{HTF} and density ρ_{HTF}. The duct geometry is characterized by the hydraulic diameter d_h and the cross-sectional area A_{flow} of the duct. Values for f_{Re}, the product of the Fanning friction factor and Reynolds number, can be found for various duct geometries in the literature [3].

$$dp_{HTF} = \frac{\dot{m}_{HTF}}{n_{ducts}} \cdot \frac{\eta_{HTF} \cdot (L_1 + L_6) \cdot 4 \cdot f_{Re}}{2 \cdot d_h^2 \cdot \rho_{HTF} \cdot A_{flow}} \quad (5)$$

A benchmark comparison with detailed CFD simulations of the TES designed for the pilot plant showed a deviation of less than 3.5% of the charging and discharging time for an entire cycle while requiring orders of magnitude less computational effort, which is suitable for dynamic process simulations.

2.2 Solar Absorbing Gas Receiver Model

The considered cavity receiver uses the ability of some gases to absorb a significant fraction of longer wavelength thermal radiation while being mostly transparent to terrestrial solar radiation, e.g. carbon dioxide or water vapour [4]. In the pilot plant, steam is used as HTF, which enters the receiver cavity through the front and exits through the back. It absorbs the infrared radiation emitted by the cavity surfaces, which are heated by solar radiation passing through the aperture. This receiver has been modeled in detail using CFD simulations [5], but that model is not suitable for dynamic process simulations of the entire plant. Hence, a new model has been developed in Modelica. It is structured as a cylinder with a front side consisting of the aperture and front ring models, the rear side consisting of the back plate and HTF outlet models and an outer shell model for the insulation (cf. Figure 3). The concentrated solar flux $\dot{Q}_{solar}$ is an external input that can be coupled with historical or forecasted weather data via a heliostat model. Its distribution of the absorbed flux on the receiver surfaces is derived from a detailed CFD and raytracing simulation. These simulations showed that the HTF absorbs less than 2% of the solar radiation. Any solar input for the Modelica model is propagated to the respective sub-model according to the normalized distribution of the CFD results and heats the respective cavity wall or HTF.

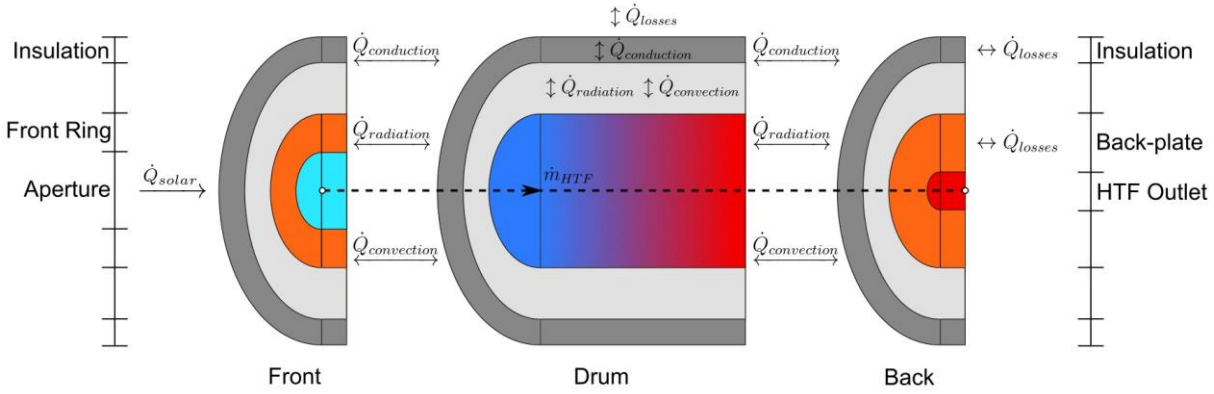

Figure 3. *Conceptual diagram of the reformer model*

The wall-to-HTF radiation exchange is modeled as a balance of the surface brightnesses $\dot{Q}_{surface}$ at the boundaries between the HTF model and the respective gray surface i, e.g the drum or back cavity wall, with its emission coefficient ϵ_i. The HTF surface brightness consists of its own emission and the transmitted radiation from the other boundary surfaces since the medium is assumed to be non-scattering.

$$\dot{\dot{Q}}_{radiation,i} = \dot{Q}_{surface,i\rightarrow HTF} - \dot{Q}_{surface,HTF\rightarrow i} \tag{6}$$

$$\dot{Q}_{surface,HTF\rightarrow i} = A_i \cdot \sigma \cdot \epsilon_{HTF,i} \cdot T_{HTF}^4 + \sum_j \dot{Q}_{transmission,j\rightarrow i} \tag{7}$$

$$\dot{\dot{Q}}_{surface,i\rightarrow HTF} = A_i \cdot \sigma \cdot \epsilon_{surface,i} \cdot T_{surface,i}^4 + (1-\epsilon_i) \cdot \dot{Q}_{surface,HTF\rightarrow i} \tag{8}$$

The total emissivity of the HTF volume at the average HTF temperature towards a surface ϵ_i is modeled with the weighted sum of gray gas model (WSGGM), which assumes that the total emissivity of the medium can be calculated as the sum of m gray gases with a temperature-dependent weighting factor $w_{\epsilon,m}$. The mean beam length $L_{HTF\rightarrow i}$ from a gas volume towards its boundary surface can be found in the literature for various configurations [6].

$$\epsilon_{HTF,i} = \sum_m w_{\epsilon,m}(T_{HTF}) \cdot (1 - e^{-\kappa_m \cdot L_{HTF\rightarrow i}}) \tag{9}$$

The transmitted radiation is calculated with the Beer-Lambert law and view factors $F_{j\rightarrow i}$ from surface j and i [7]. The attenuation coefficient κ can be obtained via the WSGGM and the mean optical path length $l_{j\rightarrow i}$ between the respective surfaces.

$$\dot{\dot{Q}}_{transmission,j\rightarrow i} \cdot A_i = \dot{Q}_{surface,i\rightarrow HTF} \cdot A_j \cdot F_{j\rightarrow i} \cdot e^{\kappa \cdot l_{j\rightarrow i}} \tag{10}$$

The major energy influx into the HTF occurs due to radiation, but convection is also modeled with a Nusselt correlation for the various surfaces while the HTF passes them. Together with the HTF enthalpy flow balance $\Delta\dot{H}_{HTF}$, this results in the following overall HTF energy balance:

$$m_{HTF} \cdot c_{p,HTF} \cdot \frac{dT_{HTF}}{dt} = \Delta\dot{H}_{HTF} + \sum_i \dot{Q}_{radiation,i} + \sum_i \dot{Q}_{convection,i} \tag{11}$$

The surface temperatures are coupled to the environment via thermal conduction through the insulation shell and back plate. $\dot{Q}_{conduction}$ and subsequent convective and radiative heat losses on the outer receiver surfaces $\dot{Q}_{losses}$. The model results pass the plausibility tests regarding the receiver output temperature. Still, they should be validated with experimental

data since the geometrical simplification to a cylindrical drum fromthe actual receiver geometry is significant. However, modeling it in detail would drastically decrease the numerical performance which is paramount for the process simulation.

2.3 Reformer Model

Key to modeling the reformer is the modeling of the thermochemical reactions. The main reactions occurring in the reforming reactor for the solar fuel synthesis are steam methane reforming (SRM), carbon dioxide reforming (CDR) and the water-gas shift reaction (WGS). A suitable simplification is disregarding the reaction kinetics and determining the thermochemical equilibrium (TCE). The reaction system is characterized by composition, temperature and pressure and the Gibbs free energy minimization is applied to determine the output composition of the reformer. This has proven to be a robust and effective method in the chemical industry [8, 9] and can be implemented as equations in Modelica. At the equilibrium state, the total Gibbs free energy G is minimal. Therefore, its differential dG is zero for the system temperature T and system pressure p. It is defined as:

$$(dG)_{T,p} = \sum_{j=1}^{NS} \mu_j dN_j = 0 \tag{12}$$

μ_j is the chemical potential of species j, N_j is the molar amount of species j and *NS* is the total number of species. The chemical potential is represented for ideal gases by the following equations:

$$\mu_j = \left(\frac{\partial g}{\partial N_j}\right)_{p,T,N_i} = h_{f,j}^0 + \left(h_j - h_j^0\right) - Ts_j^0 - RTln\left(\frac{p_j}{p_0}\right) \tag{13}$$

$$\ln\left(\frac{p_j}{p_0}\right) = \ln\left(\frac{N_j}{N}\right) + \ln\left(\frac{p}{p_0}\right) \tag{14}$$

$h_{f,j}^0$ is the enthalpy of formation at reference temperature T_0, h_j is the enthalpy at system temperature, h_j^0 is the enthalpy at reference temperature, s_j^0 is the entropy at system temperature at reference pressure p_0, R is the gas constant, p_j is the partial pressure and N is the total molar amount in the system. The chemical potential is determined for each species occurring in the aforementioned reactions: $j = \{CH_4, CO_2, CO, H_2O, H_2\}$.

In order to solve this stiff mathematical problem, the method of Lagrange Multipliers is a common technique [8, 10]. As a first step, the formulation of constraint conditions for N_j is necessary. The conservation of mass, meaning that the molar amount for each element i in the system must remain constant, yields the following constraint condition:

$$\varphi_i = 0 = \sum_{j=1}^{NS} a_{i,j} N_j - b_i \tag{15}$$

b_i is the molar amount of element *i* in the system and $a_{i,j}$ is the number of atoms of element i per molecule of species j. This results in $NE = 3$ conditions for each element $i = \{H, C, O\}$ in the system under consideration. Furthermore, the sum of all molar amounts for each species is equal to the total molar amount in the system, which results in this condition:

$$0 = \sum_{j=1}^{NS} N_j - N \tag{16}$$

The Lagrange function La is given with the Lagrange multipliers λ_i as:

$$La = G(N_j) + \sum_{i=1}^{NE} \lambda_i \cdot \varphi_i \tag{17}$$

Differentiating La with respect to N_j yields the *NS* missing equations for each species j:

$$0 = \mu_j + \sum_{i=1}^{NE} \lambda_i a_{i,j} \tag{18}$$

The input for the chemical equilibrium calculation $\dot{Q}_{in}$ is the heat flow from the HTF, which is the sum of the heat flow rate heating the gas $\dot{Q}_{heating}$ and the heat flow rate needed for the reaction $\dot{Q}_{reaction}$. Those are determined with the input and output conditions of the reaction system, which are the specific gas enthalpy h at temperature T and composition X, the total molar mass M, the molar flow rate $\dot{n}$ and the volume flow $\dot{V}$:

$$\dot{Q}_{heating} = M_{in}\dot{n}_{in} \cdot [h(T_{out}, X_{in}) - h(T_{in}, X_{in})] \tag{19}$$

$$\dot{Q}_{reaction} = M_{out}\dot{n}_{out} \cdot h(T_{out}, X_{out}) - M_{in}\dot{n}_{in} \cdot h(T_{out}, X_{in}) - p \cdot (\dot{V}_{out} - \dot{V}_{in}) \tag{20}$$

In order to get a computationally efficient model of the reformer, it is simplified to a pseudo-homogenous one-dimensional system, i.e. the reactant gas volume has a homogeneous velocity, pressure, composition and temperature. The gradient in internal energy $(dU)_T$ is neglected as well. This assumption warrants the reformer to be discretized into smaller sub-volumes to reduce the differences between input and output conditions. The heat transfer from the HTF depends on the reformer design and can be implemented similarly to the TES model. Comparisons have shown a good agreement between the experimental reformer output compositions and the calculated TCE at 10 K below the output temperature.

3. Interfaces with other open-source software

Modelica possesses interfaces to various external environments. An external simulation model can be either implemented in the Modelica environment as a Functional Mock-up Unit (FMU), or the Modelica model itself can be exported as an FMU. An example of the FMU approach is the implementation of thermochemical calculations. They can be implemented manually as described in 2.3 or a Python FMU can be used to access chemical simulation tools, e.g. the Cantera library. It offers an efficient way to quickly create a model but suffers from a comparably longer computation time due to the FMU interface between Modelica and Python. The FMU was initially used in the process model development, but was later replaced with the model outlined in 2.3.

Another way to create a Python-Modelica interface is using the Python library ModelicaRes to run Modelica simulations, whose in- and outputs can be coupled with other Python libraries. This enables the use of optimizing algorithms like Nelder-Mead, e.g. to optimize parameters of a model [11]. An application of this would be the fitting of models with validation data, e.g. the mean optical path lengths of the receiver can be set as a parameter to be fitted to the experimental data to model the actual receiver geometry more accurately.

4. Conclusion & Outlook

A complex process model covering the solar fuels synthesis process, considering thermohydraulic and radiative interactions as well as thermochemical reactions, was developed within the Modelica framework. Certain simplifications and assumptions needed to be made, mainly to realize a feasible computation time of the process model. The model results showed an acceptable agreement with more detailed but slower to simulate stand-alone

models of the components in different environments. Modelica has interfaces to other open-source software, like Python, which makes third-party software integrations possible and enables the optimization of model parameters to fit experimental data for validation purposes.

This model has been developed alongside the plant engineering, aiding in the plant design and development of control strategies and parameters. The dynamic process model and this approach will be validated with experimental data of the real plant. The validated model can prospectively aid in its operation via model predictive control or operational assistance as well.

Data availability statement

The used data and specifications are subject to third-party IP and not publically available.

Author contributions

Conceptualization[1], Data curation[1], Formal Analysis[1], Funding acquisition[1,2,3,6], Investigation[1], Methodology[1,3], Project administration[1,2], Software[1,3,4,5], Supervision[2,3,6], Visualization[1], Writing – original draft[1,4], Writing – review & editing[2,3,6]

Competing interests

The authors declare that they have no competing interests.

Funding

The authors gratefully acknowledge the financial support from the German Federal Ministry for Economic Affairs and Climate Action (BMWK).

Acknowledgement

This work was carried out with financial support from the German government through its 7th Energy Research Programme (FKZ: 03EE5085C, SolarFuels). We also thank our co-workers at the German Aerospace Center (DLR) and Synhelion Germany GmbH.

References

1. C. Schwager, F. Angele, P. Schwarzbözl, C.J. Teixeira Boura, U. Herrmann, 2021. "Model Predictive Assistance for Operational Decision Making in Molten Salt Receiver Systems, " SolarPACES 2021, AIP Publishing, 2023. doi: 10.1063/5.0151514.
2. C. Rendón et al., "Modeling and upscaling of a pilot bayonet-tube reactor for indirect solar mixed methane reforming," SolarPACES 2019, AIP Publishing, 2020. doi: 10.1063/5.0029974.
3. R. K. Shah, A. L. London, and F. M. White, "Laminar Flow Forced Convection in Ducts," Journal of Fluids Engineering, vol. 102, no. 2. ASME International, pp. 256–257, Jun. 01, 1980. doi: 10.1115/1.3240677.
4. G. Ambrosetti and P. Good, "A novel approach to high temperature solar receivers with an absorbing gas as heat transfer fluid and reduced radiative losses," Solar Energy, vol. 183. Elsevier BV, pp. 521–531, May 2019. doi: 10.1016/j.solener.2019.03.004.
5. S. A. Zavattoni, D. Montorfano, P. Good, G. Ambrosetti, and M. C. Barbato, "The synhelion absorbing gas solar receiver for 1'500 °C process heat: CFD modeling," SolarPACES 2019, AIP Publishing, 2020. doi: 10.1063/5.0029314.

6. M. F. Modest, "Solution Methods for Nongray Extinction Coefficients," Radiative Heat Transfer. Elsevier, pp. 626–693, 2013. doi: 10.1016/b978-0-12-386944-9.50020-0.
7. I. Martinez. "Radiative View Factors" Heat Transfer and Thermal Radiation Modeling. http://imartinez.etsiae.upm.es/~isidoro/tc3/Radiation%20View%20factors.pdf (accessed on 26. Sept. 2023)
8. S. Gordon, B.J. McBride, "Computer program for the calculation of Complex chemical equilibrium compositions with applications. Part 1: Analysis," NASA reference publication 1311, 1994. Link: https://ntrs.nasa.gov/citations/19950013764
9. J. Solsvik, T. Haug-Warberg, and H. A. Jakobsen, "Implementation of chemical reaction equilibrium by Gibbs and Helmholtz energies in tubular reactor models: Application to the steam–methane reforming process," Chemical Engineering Science, vol. 140. Elsevier BV, pp. 261–278, Feb. 2016. doi: 10.1016/j.ces.2015.10.011.
10. Q. Liu, C. Proust, F. Gomez, D. Luart, and C. Len, "The prediction multi-phase, multi reactant equilibria by minimizing the Gibbs energy of the system: Review of available techniques and proposal of a new method based on a Monte Carlo technique," Chemical Engineering Science, vol. 216. Elsevier BV, p. 115433, Apr. 2020. doi: 10.1016/j.ces.2019.115433.
11. J. Schulte, C. Schwager, C. Frantz, F. Schloms, C.J. Teixeira Boura, U. Herrmann, "Control Concept for a Molten Salt Receiver in Star Design: Development, Optimization and Testing with Cloud Passage Scenarios," SolarPACES 2022